Available online at www.sciencedirect.com
ScienceDirect
Tetrahedron
Tetrahedron 63 (2007) 11114–11121

The synthesis of a pyrrole-functionalized cyclobis(paraquat-*p*-phenylene) derivative and its corresponding [2]rotaxane and [2]catenane and their subsequent deposition onto an electrode surface

Graeme Cooke,[a,*] Lee M. Daniels,[b] Francine Cazier,[c] James F. Garety,[a] Shanika Gunatilaka Hewage,[a] Andrew Parkin,[a] Gouher Rabani,[a] Vincent M. Rotello,[d] Chick C. Wilson[a] and Patrice Woisel[e,*]

[a]*WestCHEM, Department of Chemistry, Joseph Black Building, University of Glasgow, Glasgow, Scotland G12 8QQ, UK*
[b]*Rigaku, 9009 New Trails Drive, The Woodlands, TX 77381, USA*
[c]*Laboratoire de Synthèse Organique et Environnement, Université du Littoral Côte d' Opale, Dunkerque 59140, France*
[d]*Department of Chemistry, University of Massachusetts at Amherst, Amherst, MA 01002, USA*
[e]*Laboratoire de Chimie Organique et Macromoléculaire UMR-CNRS 8009, Université des Sciences et Technologies de Lille, Villeneuve d'Ascq 59655, France*

Received 29 May 2007; revised 23 July 2007; accepted 8 August 2007
Available online 14 August 2007

Abstract—We report the convenient synthesis of a pyrrole-functionalized tetracationic cyclophane, [2]rotaxane, and [2]catenane. X-ray crystallography has confirmed the interlocked structure of the catenane. We have investigated the solution properties of these systems using solution electrochemistry, NMR, and UV–vis spectroscopy. We have also demonstrated that it is possible to immobilize these systems onto a platinum working electrode surface. We have shown that films of the cyclophane have the ability to undergo complexation with a dialkyloxynaphthalene derivative.

1. Introduction

Rotaxanes and catenanes incorporating the tetracationic cyclophane cyclobis(paraquat-*p*-phenylene)($CBPQT^{4+}$)[1] have undoubtedly become important supramolecular building blocks for the construction of molecular-scale machines and devices.[2] In attempts to facilitate their future applications, attention has focused upon the transferral of these systems from solution to the solid state, where the resulting surface-confined assemblies have the ability to function coherently.[3] For the most part, the transferal has been achieved by the fabrication of self-assembled monolayers onto a range of solid substrates. As an alternative strategy for depositing components onto surfaces, electropolymerization of systems functionalized with polymerizable units (e.g., thiophene and pyrrole) offers a convenient and versatile method for surface deposition. Furthermore, as the polymerization process provides a conjugated backbone with interesting physical properties, this method not only facilitates communication between the components of the film, but also should facilitate the molecular electronics and device applications of these systems.[4] As part of our continuing exploration of using electropolymerization to immobilize interlocked structures onto surfaces,[4f,5] we now report a convenient synthetic route to introduce electro-active pyrrole moieties into cyclophane **1**[6] and its corresponding [2]rotaxane **2** and [2]catenane **3**. We also report a convenient method of depositing these species onto an electrode surface.

2. Results and discussion

2.1. Synthesis

The synthesis of compounds **1**,[6] **2**, and **3** is given in Scheme 1. Key building block **5** was readily synthesized from 1-*N*-pyrrolepropionic acid[7] and alcohol **4**.[6] Cyclophane **1** was synthesized from compounds **5** and **6** using a template directed clipping methodology using **7**.[8,9] Rotaxane **2** and catenane **3** were also readily synthesized using this methodology by replacing template **7** with axle **8**[9] or macrocycle **9**,[10] respectively. The cyclophane **1** and interlocked

* Corresponding authors. E-mail: graemec@chem.gla.ac.uk

0040–4020/$ - see front matter © 2007 Elsevier Ltd. All rights reserved.
doi:10.1016/j.tet.2007.08.027

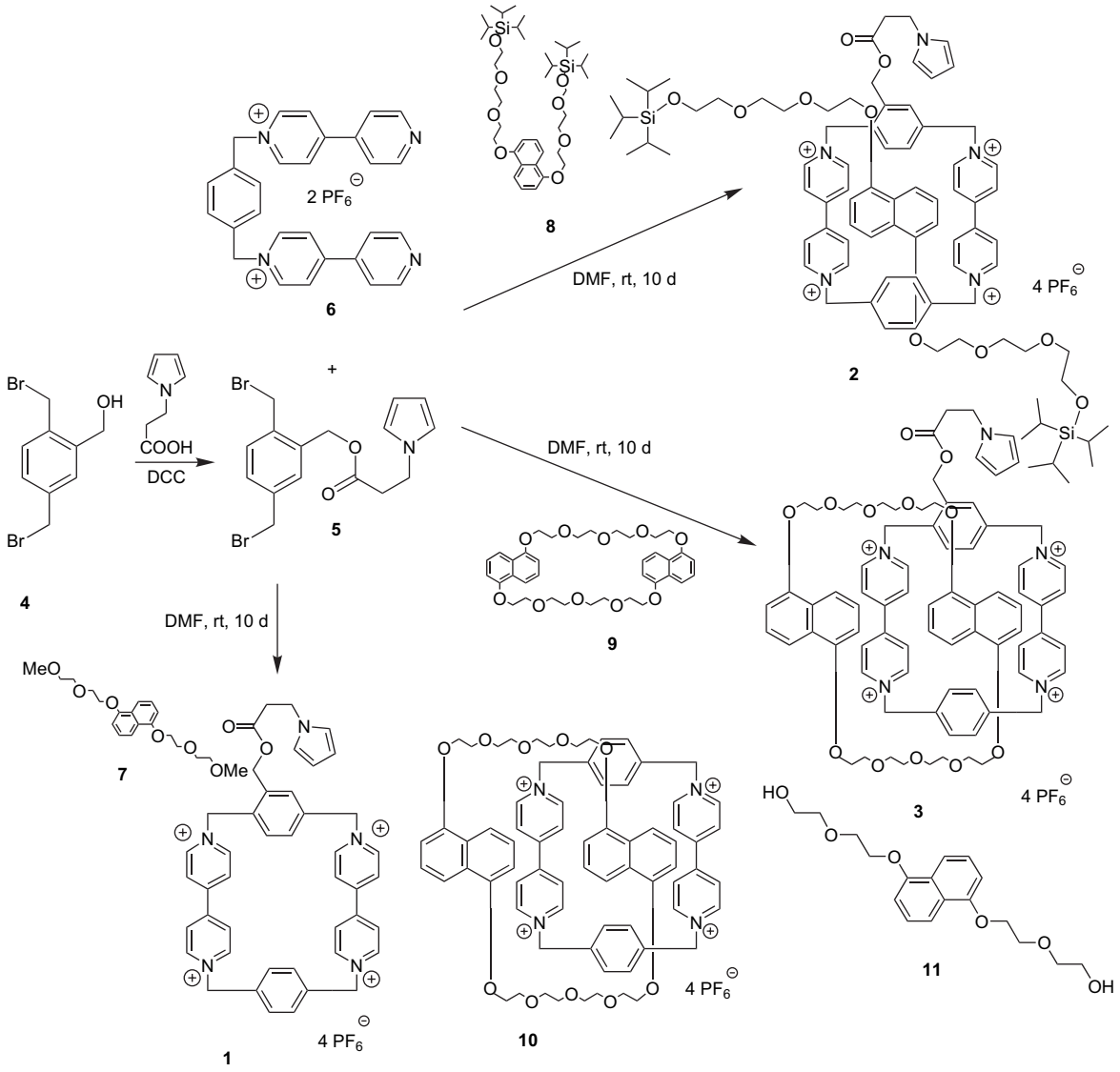

Scheme 1. Synthesis of cyclophane **1**, rotaxane **2**, and catenane **3**.

structures **2** and **3** were purified by column chromatography (SiO_2, $MeOH/NH_4Cl/MeNO_2$). The Cl^- counterions were converted to PF_6^- by exchange reactions with NH_4PF_6 to yield structures **1**–**3**. The analytical data for systems **2** and **3** were consistent with their proposed structures. For example, electrospray mass spectrometry performed on **2** and **3** revealed peaks at m/z=1843 $[M-PF_6]^+$ and 1743 $[M-PF_6]^+$, respectively.

2.2. Solid state structure of 3

Crystals suitable for study by X-ray diffraction were obtained by the slow evaporation of solvent from a concentrated solution of **3** in acetonitrile. Although the crystals were of poor quality, a crystal structure was obtained using a Rigaku R-AXIS RAPID image-plate diffractometer, affording data of sufficient quality to solve and refine the structure from a long data collection in which each image was exposed for a total of 35 min. This type of laboratory image plate set-up is particularly powerful for small, weakly diffracting crystals such as this as it allows for very long exposure times without the dark-current build-up associated with CCD detectors. The crystal structure clearly shows a highly ordered molecular arrangement within the catenane architecture (Fig. 1). One of the 1,5-dinaphtho- residues is sandwiched between the two bipyridinium moieties of the tetracationic cyclophane, whereas the other unit is positioned outside and immediately adjacent to one of the bipyridinium units.[11] It is noteworthy that the naphthalene and bipyridinium aromatic rings adopt a near parallel arrangement, whereas the electron rich pyrrole moiety does not apparently interact significantly with the interlocked structure in the solid state.

2.3. Characterization of 1, 2, and 3 in solution

The solution properties of **1** have been described previously.[6] The absorption spectra recorded in CH_3CN at 298 K, show a broad band in the visible region for both interlocked structures **2** and **3** at 524 and 530 nm, respectively. Inspection of the ^1H NMR spectra of **2** and **3** performed in CD_3CN, showed two characteristic proton resonances at

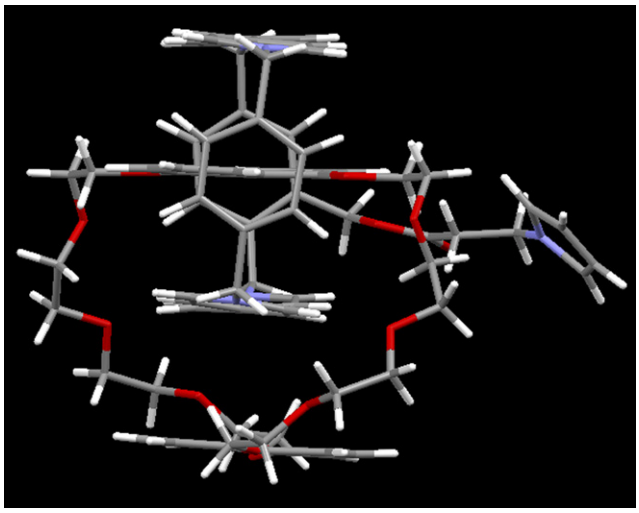

Figure 1. X-ray crystal structure of catenane **3**.

δ=6.2 and 6.7 ppm for the protons of the pyrrole moiety. A notable feature in the ^{1}H NMR spectra is the significant upfield position of the resonances of the 1,5-dialkyloxynaphthalene protons of **2** and **3**, compared to the same protons of the corresponding free templates **8** and **9**. This is particularly evident for the resonance of the protons attached to the 4- and 8-position, which is shifted by $\Delta\delta \approx 5.3$ ppm for both interlocked structures.

We have investigated the solution electrochemistry of cyclophane **1** and interlocked structures **2** and **3** in acetonitrile (see Fig. 2). Cyclophane **1** displayed electrochemical data consistent with the tetracationic cyclophane, and gave rise to two reversible reduction waves corresponding to the formation of the diradical dication and fully reduced states.[6,12] Rotaxane **2** displays two one-electron reduction waves and a one two-electron reduction wave in accordance with previously reported systems.[13] The interlocked system **3** displays more complicated electrochemical behavior than the related system **10**, which lacks a pyrrole functionality attached to the CBPQT^{4+} unit.[11] When the CV data for **3** and cyclophane **1** are compared, it is clear that catenation of **1** by the electron rich **9** results in the formation of four one-electron reduction waves; the first and the second pair of waves are shifted to more negative potentials than the redox waves observed for the formation of the diradical dication and fully reduced states of **1**. This negative shift in the redox waves of **3** is presumably due to donor–acceptor interactions destabilizing the reduced states of the CBPQT^{4+} unit.[12] Furthermore, comparison of this electrochemical data to that reported for catenane **10**,[11] suggests that the formation of four destabilized reduced states of the CBPQT^{4+} units is presumably due to the influence of the electron rich pyrrole unit in the side chain.

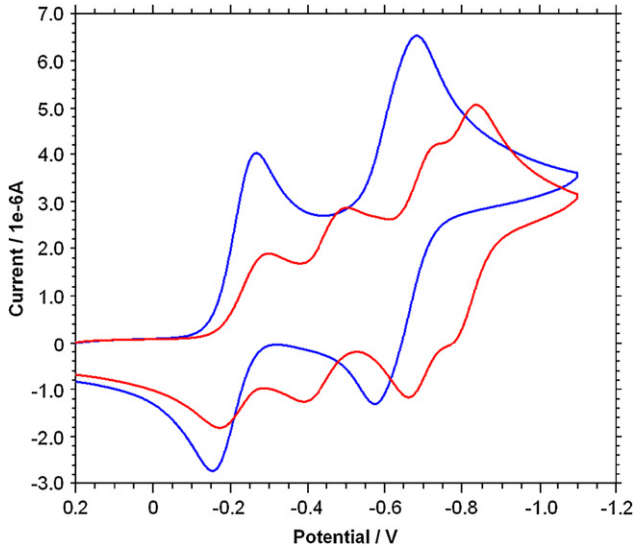

Figure 2. Cyclic voltammograms of **3** ($\sim 3\times10^{-4}$ M) — and **1** ($\sim 3\times10^{-4}$ M) — in acetonitrile (0.1 M Bu_4NPF_6). Scan rate=0.1 V s^{-1}.

2.4. Deposition onto surfaces

We next investigated whether systems **1**, **2** or **3** could be deposited onto an electrode surface. Functionalized electrodes have successfully been formed by cycling the potential applied to separate solutions of **1**, **2** or **3** (see Figs. 3–5). In particular, using similar methodology devised for the polymerization of viologen functionalized pyrrole derivatives, derivatives **1**–**3** could be deposited onto an electrode surface

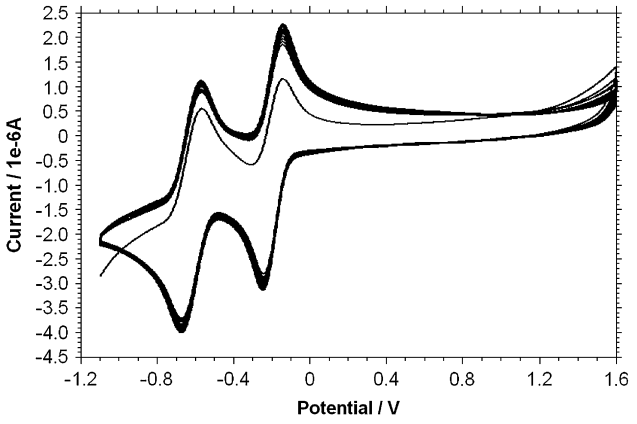

Figure 3. CV showing repeated redox cycles of **1** in a $\sim 2\times10^{-4}$ M solution in acetonitrile. The CV shows 16 cycles between −1.1 and +1.6 V. Scan rate=0.1 V s^{-1}.

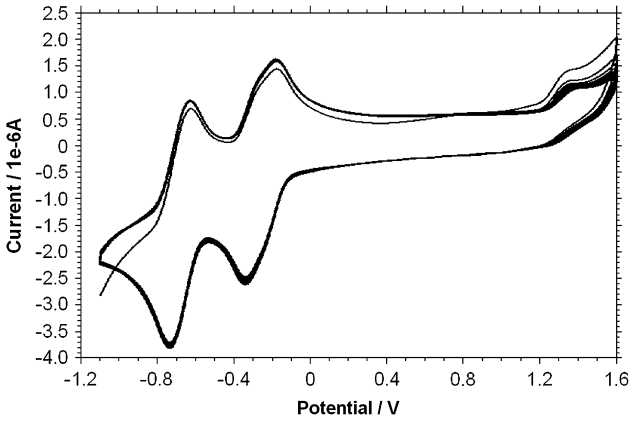

Figure 4. CV showing repeated redox cycles of **2** in a $\sim 2\times10^{-4}$ M solution in acetonitrile. The CV shows 16 cycles between −1.1 and +1.6 V. Scan rate=0.1 V s^{-1}.

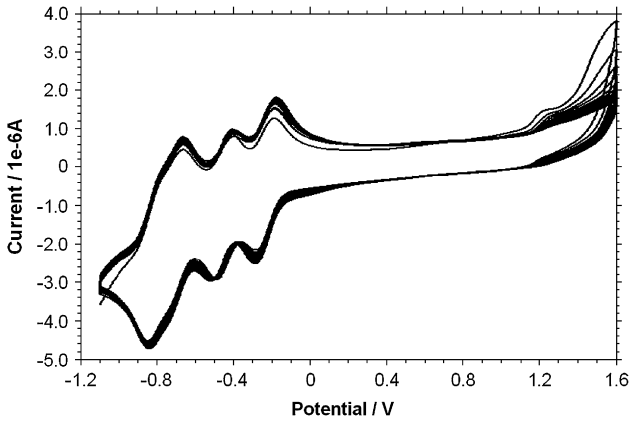

Figure 5. CV showing repeated redox cycles of **3** in a ~2×10^{-4} M solution in acetonitrile. The CV shows 16 cycles between −1.1 and +1.6 V. Scan rate=0.1 V s^{-1}.

(from a solution in acetonitrile) by cycling the applied potential between −1.1 and +1.6 V.[14] Although evidence for the polymerization of derivatives was obtained by monitoring the increase in current for the reduction waves of the cyclophane following subsequent electrochemical cycles, there was no evidence for a new redox wave being formed resulting from the electrosynthesis of a polypyrrole backbone. Furthermore, the increase in current for the reduction waves for the cyclophane unit during repeated electrochemical cycling appears to stop after a few redox cycles, thereby indicating the formation of at best short oligomers on the electrode surface. Moreover, rotaxane **2** appears to be the most difficult structure to deposit as only limited growth of the redox waves was observed, presumably due to the bulky nature of this interlocked system and the likely associated Coulombic repulsion inherent in $CBPQT^{4+}$ polymers of this type. The redox wave at around +1.3 to +1.4 V for the interlocked structures has been attributed to the oxidation of the naphthalene units of these systems.[15]

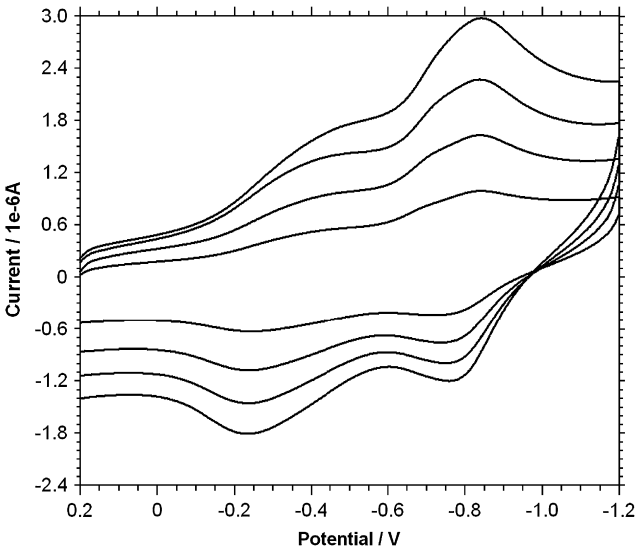

Figure 7. CV studies showing the reduction of films of **2** in acetonitrile. Films were fabricated from a ~2×10^{-4} M solution of **2** in acetonitrile. Scan rate=1 V s^{-1} (largest current), 0.75, 0.50, 0.25 V s^{-1} (smallest current). $\Gamma=1\times10^{-11}$ mol cm^{-2}.

Following deposition, the functionalized working electrodes were washed with acetone, and the films were allowed to dry in air for about 1 h. The functionalized electrodes were then placed into a fresh electrolyte solution (0.1 M solution of Bu_4NPF_6 in acetonitrile) and their electrochemistry was investigated using CV (see Figs. 6–8). Using freshly prepared functionalized electrodes, reductive scans between +0.2 and −1.2 V were recorded, which revealed redox waves due to reduction of the cyclophane moieties and thus provided clear evidence for the cyclophane moiety being deposited onto the surface. It is noteworthy, particularly for immobilized **1** and **3**, that the deposition process imposes a new electrochemical environment on the cyclophane moieties, as evidenced by the differing electrochemical data observed for the

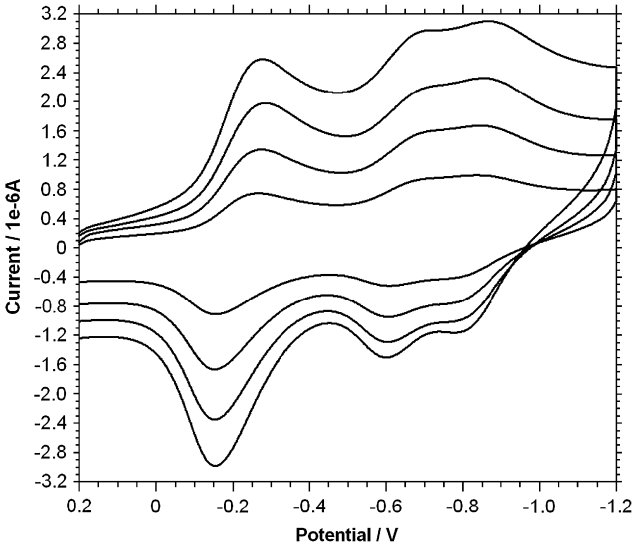

Figure 6. CV studies showing the reduction of films of **1** in acetonitrile. Films were fabricated from a ~2×10^{-4} M solution of **1** in acetonitrile. Scan rate=1 V s^{-1} (largest current), 0.75, 0.50, 0.25 V s^{-1} (smallest current). $\Gamma=4\times10^{-11}$ mol cm^{-2}.

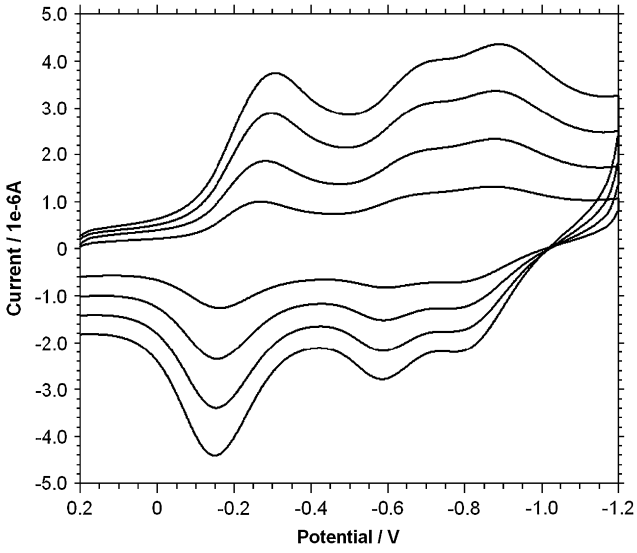

Figure 8. CV studies showing the reduction of films of **3** in acetonitrile. Films were fabricated from a ~2×10^{-4} M solution of **3** in acetonitrile. Scan rate=1 V s^{-1} (largest current), 0.75, 0.50, 0.25 V s^{-1} (smallest current). $\Gamma=6\times10^{-11}$ mol cm^{-2}.

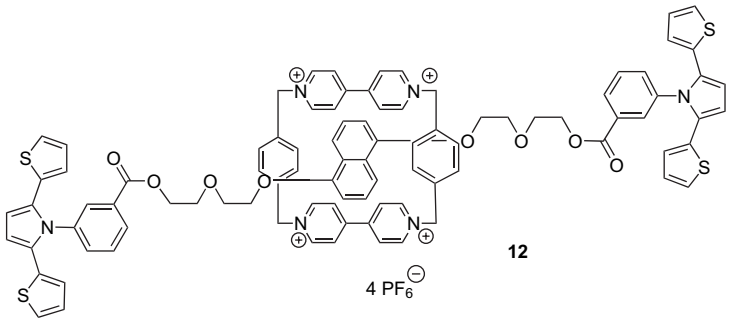

cyclophane reduction waves to that observed in solution. This differing electrochemical data is likely to be due to the enforced close proximity of the cyclophane units in the films. Surface-confined behavior of the redox-active moieties was confirmed by recording the CVs of the thin films of **1**–**3** at different scan rates, as a linear increase in current with scan rate for the reduction processes of the cyclophane was observed. The films of the deposited derivatives proved to be reasonably stable, displaying a similar current/voltage response for more than 10 scan cycles. The estimated surface coverage (Γ) for films of **1**–**3** suggests sub-monolayer coverage, which is in accordance with the CV data observed during the deposition process.

In a previous paper, we reported the deposition of derivative **12** from a 1:1 acetonitrile/toluene solution onto a working electrode surface by repeated oxidation of the dithienylpyrrole stopper units.[4f] We now report an improved method for depositing this derivative, which prevents problems associated with the over oxidation of the growing polymer backbone and toluene during this process.[16] When the scan potentials were reduced to between 0 and +1.4 V, a new pseudoreversible redox wave was developed at +0.7 V and an irreversible wave developed at ~+0.3 V upon repeated redox cycling, which is presumably due to the developing polymeric backbone (Fig. 9). The electrochemistry of the washed (acetone) and dried functionalized electrodes was recorded in acetonitrile, which gave rise to a two-electron reduction wave and two one-electron reduction waves, presumably corresponding to the formation of the radical dication and fully reduced states for the electron deficient cyclophane (Fig. 10). We have also investigated the electropolymerisation of **12** under the conditions used for the deposition of **1**–**3**. Clear evidence of surface deposition of **12** was observed (Fig. 11), and in accordance with the data observed

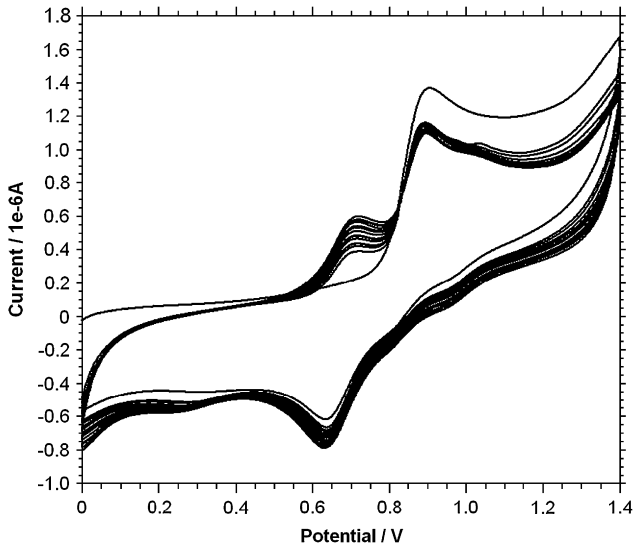

Figure 9. CV studies showing repeated redox cycles (16 scans) of **12** (1×10^{-4} M solution in acetonitrile/toluene 1:1 (v/v)). Scan rate=0.1 V s^{-1}.

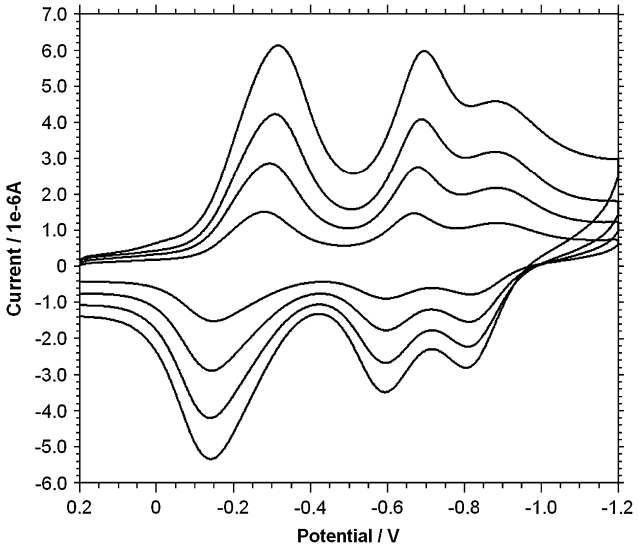

Figure 10. CV studies showing reduction of films of **12** in acetonitrile. Films were fabricated from a ~1×10^{-4} M solution of **12** in acetonitrile/toluene (1:1, v/v). Scan rate=1 V s^{-1} (largest current), 0.75, 0.50, 0.25 V s^{-1} (smallest current). $\Gamma=2\times10^{-10}$ mol cm^{-2}.

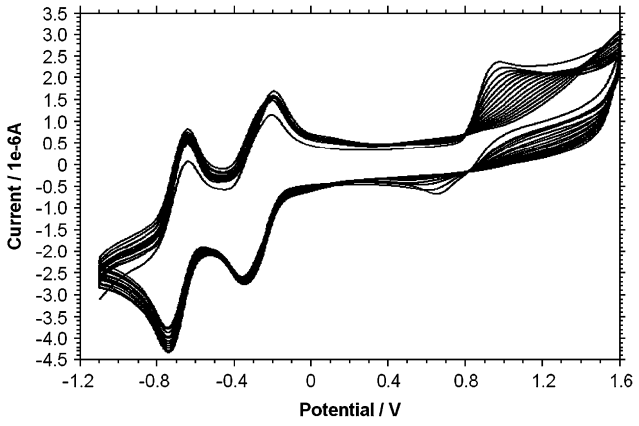

Figure 11. CV showing repeated redox cycles of **12** in a ~2×10^{-4} M solution in acetonitrile. The CV shows 16 cycles between −1.1 and +1.6 V. Scan rate=0.1 V s^{-1}.

for the deposition of derivatives **1**–**3**, cyclic voltammetry indicates that short oligomers are being deposited onto the electrode surface (Fig. 12). The surface coverage (Γ=8×10^{-11} mol cm^{-2}) was around an order of magnitude less for this method compared to that values obtained from the cyclic voltammograms shown in Figure 10 (Γ=2×10^{-10} mol cm^{-2}).

Finally, we have investigated the complexation properties of films of cyclophane **1**, and in particular, the effect the addition of guest **11** has on the electrochemical properties of the cyclophane moiety.[17] Addition of **11** to the electrolyte solution immediately resulted in the first redox wave of the cyclophane being shifted to more negative values (~60 mV). We attribute this destabilization of the diradical dication state of the cyclophane to the donor–acceptor interactions

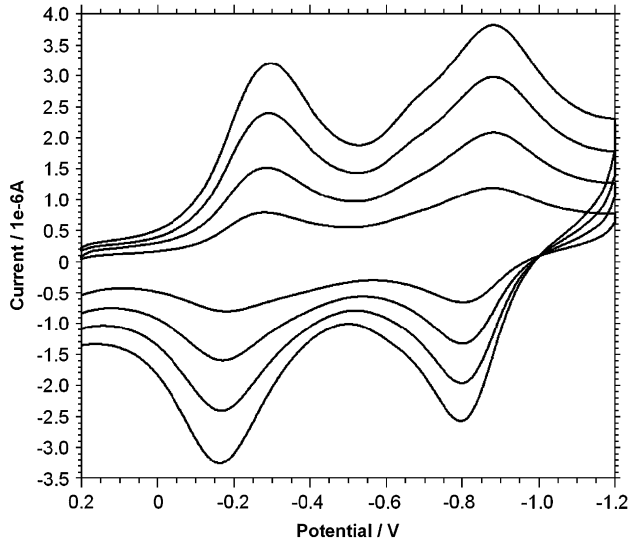

Figure 12. CV studies showing reduction of films of **12** in acetonitrile. Films were fabricated from a ~2×10^{-4} M solution of **12** in acetonitrile. Scan rate=1 V s^{-1} (largest current), 0.75, 0.50, 0.25 V s^{-1} (smallest current). Γ=8×10^{-11} mol cm^{-2}.

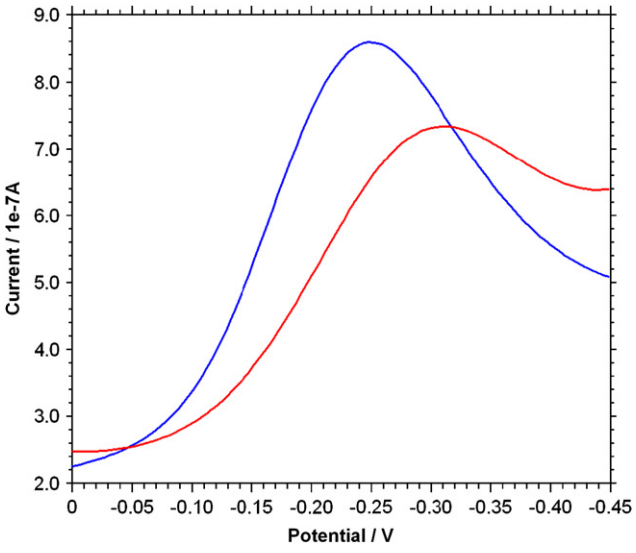

Figure 13. Square wave voltammograms of films of **1** — and in the presence of **11** (~2×10^{-2} M) — recorded in acetonitrile.

resulting from complex formation between the naphthalene and cyclophane moieties (Fig. 13). This is consistent with electrochemical data observed for CBPQT^{4+}-based systems in acetonitrile solution, and indicates that complex formation occurs between the immobilized cyclophane moieties of **1** and **11**.[12]

3. Conclusions

In conclusion, we have shown that compound **1** and its corresponding interlocked structures **2** and **3** can be deposited onto electrode surfaces. Although the electrochemical data suggest that at best short oligomers are formed, electrochemical measurements performed on the resulting films suggest that they are reasonably robust. We have also shown that thin films of **1** are capable of complexation with **11**. Work is underway in our laboratory to investigate the molecular electronic properties of these systems, and develop the next generation of systems with improved electropolymerisation properties. The results from these studies will be reported in due course.

4. Experimental

4.1. General synthesis

Solvents were purified and dried by literature methods. Compounds **4**,[6] **5**,[6] **6**,[12] **7**,[8] **8**,[9] **9**,[10] **11**,[18] and **12**[4f] were synthesized according to the literature methods.

4.1.1. Synthesis of 4. A mixture of DIBAL-H (18.3 mL, 1 M in toluene) and toluene (10 mL) was cooled to 0 °C under nitrogen. A solution of ethyl 2,5-bis(bromomethyl)benzoate (2.9 g, 8.73 mmol) in toluene (20 mL) was added dropwise, and the reaction mixture was stirred for 3 h at 0 °C. Hydrochloric acid (1 M) was added (until pH=1 was reached), and the organic phase was extracted, washed with water, dried over Na_2SO_4, and filtered. The solvent was evaporated and the product was washed with ice-cold ether to yield **4**; yield: 90%; mp 124–125 °C. ^{1}H NMR ($CDCl_3$, 250 MHz, 298 K): δ=7.50 (s, 1H), 7.33 (m, 2H), 4.87 (s, 2H), 4.63 (s, 2H), 4.51 (s, 2H), 1.75 (br s, 1H); ^{13}C NMR ($CDCl_3$, 75 MHz, 298 K): δ=35.8, 38.5, 66.1, 133.3, 134.0, 136.0, 140.4, 143.5, 146.5. MS (EI): *m*/*z*=294 [M]$^+$ (100). Elemental analysis calcd (%) for $C_9H_{10}Br_2O$: C, 36.77; H, 3.43. Found: C, 36.96; H, 3.62.

4.1.2. Synthesis of 5. A solution of the alcohol **4** (0.5 g, 1.70 mmol), *N*-pyrrolepropionic acid (0.24 g, 1.70 mmol), 1,3-dicyclohexylcarbodiimide (0.35 g, 1.70 mmol), and 4-dimethylaminopyridine (catalytic amount) in CH_2Cl_2 (50 mL) was stirred for 3 h at room temperature. The resulting suspension was filtered, and the filtrate was evaporated and subjected to column chromatography (SiO_2: petroleum ether/EtOAc, 9:1) to furnish compound **5** as a thick oil; yield: 69%. ^{1}H NMR ($CDCl_3$, 250 MHz, 298 K): δ=7.39 (s, 2H), 7.37 (s, 1H), 6.67 (t, *J*=2 Hz, 2H), 6.17 (t, *J*=2 Hz, 2H), 5.28 (s, 2H), 4.52 (s, 2H), 4.49 (s, 2H), 4.26 (t, *J*=7 Hz, 2H), 2.87 (t, *J*=7 Hz, 2H); ^{13}C NMR ($CDCl_3$, 75 MHz, 298 K): δ= 29.9, 32.5, 36.7, 45.0, 63.5, 108.6, 129.8, 130.8, 131.3, 134.7, 136.6, 138.8, 170.9. MS (ES): *m*/*z*=438 [M+Na]$^+$(100).

Elemental analysis calcd (%) for $C_{16}H_{17}Br_2NO_2$: C, 46.29; H, 4.13. Found: C, 46.39; H, 4.07.

4.1.3. Synthesis of 1. A solution of **5** (0.52 g, 1.24 mmol), **6** (0.88 g, 1.24 mmol), and the naphthalene template **7** (1.35 g, 3.72 mmol) in dry DMF (30 mL) was stirred at room temperature for 10 days. The solvent was removed under vacuum and the residue was subjected to a liquid–liquid extraction ($CHCl_3/H_2O$). The aqueous layer was concentrated and the residue was purified using column chromatography (SiO_2: MeOH/NH_4Cl (2 M)/$MeNO_2$, 4:4:2). The fractions containing the product were combined together and concentrated in vacuo. The residue was dissolved in hot water and an aqueous NH_4PF_6 solution was added to furnish **1**. The precipitate was collected by filtration, washed with water and Et_2O, and finally dried under vacuum, yielding **1** as an orange-red solid; yield: 21%. ^{1}H NMR (CD_3CN, 400 MHz, 298 K): δ=8.94 (m, 4H), 8.76 (br d, J=6 Hz, 4H), 8.10 (br d, J=5 Hz, 2H), 7.94–7.82 (m, 9H), 7.76–7.69 (m, 4H), 5.86 (s, 2H), 5.81 (s, 2H), 5.77 (s, 2H), 5.67 (s, 2H), 5.31 (s, 2H), 3.90 (t, J=2 Hz, 2H), 3.65–3.67 (m, 2H), 3.48 (t, J=2 Hz, 2H), 2.20 (m, 2H+H_2O); ^{13}C NMR (CD_3CN, MHz, 298 K): δ=37.3, 45.2, 62.5, 64.2, 65.4, 65.6, 65.8, 108.3, 120.0, 127.4, 127.7, 127.9, 128.4, 131.5, 131.8, 132.0, 134.8, 135.2, 136.4, 136.9, 137.0, 137.8, 138.1, 145.5, 145.8, 145.9, 146.4, 148.5, 149.5, 149.8, 150.2, 172.59. HRMS (ESI): *m/z* calcd $C_{44}H_{41}F_{18}N_5O_2P_3$ [M−PF_6]: 1106.7346; found: 1106.7325.

4.1.4. Synthesis of 2. A solution of **8** (2 g, 3 mmol), **6** (0.71 g, 1 mmol), and **5** (0.41 g, 1 mmol) in dry DMF (30 mL) was stirred at room temperature for 10 days. The solvent was removed under vacuum and the residue was purified using column chromatography (SiO_2: MeOH/NH_4Cl (2 M)/$MeNO_2$, 7:2:1). The fractions containing the product were combined together and concentrated under vacuo. The residue was dissolved in hot water and an aqueous NH_4PF_6 solution was added to furnish **2**. The precipitate was collected by filtration, washed with water and Et_2O, and finally dried under vacuum, yielding **2** as a purple solid; yield: 45%; mp>300 °C. ^{1}H NMR (CD_3CN, 400 MHz, 298 K): δ=9.05 (br s, 4H), 8.67 (br s, 2H), 8.57 (br s, 1H), 8.45 (br s, 1H), 7.21–7.71 (m, 7H), 7.51–7.09 (br m, 8H), 6.82 (s, 2H), 6.38–6.13 (br m, 2H), 6.12 (s, 2H), 6.08–5.31 (br m, 12H), 4.37 (t, J=6.5 Hz, 2H), 4.37–4.31 (br m, 8H), 4.29–3.90 (br m, 8H), 3.82 (t, J=5.2 Hz, 4H), 3.75–3.47 (br m, 4H), 3.02 (t, J=6.5 Hz, 2H), 2.53 (br d, 2H), 1.05–0.94 (m, 42H); ^{13}C NMR (CD_3CN, 100 MHz, 298 K): δ=11.7, 17.3, 36.4, 44.7, 61.8, 62.7, 63.0, 64.8, 65.1, 68.4, 69.7, 70.9, 71.2, 72.7, 104.3, 108.2, 108.3, 120.8, 124.4, 124.8, 126.2, 131.4, 131.6, 132.3, 133.3, 135.5, 136.5, 136.6, 136.8, 144.2, 144.9, 145.1, 145.2, 145.3, 145.7, 151.1, 171.1. MS (ESI): 1843 [M−PF_6^-]$^+$; HRMS (ESI): *m/z* calcd $C_{84}H_{113}F_{18}N_5O_{10}P_3Si_2$ [M−PF_6]: 1843.9125; found: 1843.9128.

4.1.5. Synthesis of 3. A solution of the macrocycle **9** (0.32 g, 0.6 mmol), **6** (0.10 g, 0.24 mmol), and **5** (0.13 g, 0.24 mmol) in dry DMF (15 mL) was stirred at room temperature for 10 days. The solvent was removed under vacuum and chloroform was added (20 mL). The precipitate was isolated by filtration and purified using column chromatography (SiO_2: MeOH/NH_4Cl (2 M)/$MeNO_2$, 4:4:2). The fractions containing the product were combined together and concentrated under vacuo. The residue was dissolved in hot water and an aqueous NH_4PF_6 solution was added to furnish a purple solid. The precipitate was collected by filtration, washed with water and Et_2O, and finally dried under vacuum, yielding **3** as a purple solid; yield: 63%; mp>300 °C. ^{1}H NMR (CD_3CN, 400 MHz, 303 K): δ=9.01–8.71 (br m, 4H), 8.44 (br s, 2H), 8.34 (br s, 1H), 8.28–8.18 (br m, 1H), 8.15–8.05 (br m, 1H), 8.04 (br s, 3H), 7.88 (br s, 2H), 7.82 (br s, 1H), 7.19–6.22 (br m, 14H), 6.35 (t, J=7.6 Hz, 2H), 6.14–6.09 (br m, 2H), 5.96 (br d, J=7.2 Hz, 1H), 5.89–5.74 (br m, 6H), 5.66–5.56 (m, 5H), 5.52 (t, J=7.6 Hz, 1H), 5.40 (d, J=12.4 Hz, 1H), 4.37 (t, J=4.4 Hz, 2H), 4.27 (br s, 2H), 4.22–3.63 (br m, 30H), 3.02 (t, J=6.4 Hz, 2H), 2.44 (br d, 1H), 2.28 (br d, 1H); ^{13}C NMR (CD_3CN, 100 MHz, 303 K): δ=37.4, 47.8, 62.6, 64.0, 65.8, 66.1, 68.8, 69.1, 69.2, 70.8, 71.0, 71.2, 71.6, 71.8, 72.0, 72.1, 72.3, 72.4, 121.9, 124.9, 125.3, 126.3, 126.9, 128.6, 129.3, 132.1, 132.4, 132.7, 133.3, 134.3, 136.7, 137.2, 137.7, 137.8, 144.9, 145.3, 152.1, 154.4, 154.5, 172.2. MS (ESI): 1743 [M−PF_6^-]$^+$; HRMS (ESI): *m/z* calcd $C_{80}H_{85}F_{24}N_5O_{12}P_4$ [M−PF_6]: 1743.4739; found: 1743.4739.

4.2. X-ray crystallography

Data were collected at 100 K on a small purple block-like crystal of 0.1×0.1×0.1 mm using a Rigaku R-AXIS RAPID image-plate diffractometer equipped with an Oxford Cryosystems low temperature device and using graphite monochromated sealed tube Mo Kα radiation. This type of image plate set-up is particularly powerful for small, weakly diffracting crystals such as this as it allows for very long exposure times, without the dark-current build-up associated with CCD detectors. In this case, each image was exposed for a total of 35 min to allow enough strong data to be collected to solve and refine the structure. The data were processed using FSPROCESS within the CRYSTALCLEAR program suite[19] and WINGX[20]; an absorption correction was applied using the multi-scan method of Blessing. The structure was solved using SIR92[21] and was refined against F^2 using all data with the program CRYSTALS.[22] All P and F atoms were refined anisotropically; all other non-H atoms were refined isotropically and all H atoms were placed in geometrically calculated positions and refined as riding groups. Distance restraints were applied to all P–F bond lengths, and for the few bond distances that refined to chemically unreasonable values; chemically reasonable values were determined from the Cambridge Structural Database (CSD).[23] As the structure is non-centrosymmetric, the absolute configuration was refined, but the conformation could not be determined with any degree of certainty. The images presented in this paper were prepared using Mercury (Cambridge Crystallographic Data Centre).

M=2068.64, crystal type=Monoclinic, a=27.940(2) Å, b=13.4335(11) Å, c=27.356(2) Å, β=112.934(4)°, V=9456.0(13) Å^3, T=100 K, space group Cc, Z=4, μ(Mo Kα)=0.192 mm^{-1}, 20,976 reflections collected, 12,123 unique [R(int)=0.118], which were used in all calculations. Final $R1$ was 0.1247 and $wR2$ was 0.3471 for all data. CCDC number: 649207.

4.3. Electrochemical measurements

All electrochemical experiments were performed using a CH Instruments 620A electrochemical workstation. The

electrolyte solution (0.1 M) was prepared from recrystallized Bu_4NPF_6 and dry acetonitrile and dry toluene. A three electrode configuration was used with a platinum disc (2 mm diameter) as working electrode, an Ag/AgCl reference electrode, and a platinum wire as the counter electrode. The solution was purged with nitrogen prior to recording the electrochemical data, and all measurements were recorded under a nitrogen atmosphere.

The cyclophane-modified electrodes were washed thoroughly with acetone and dried in air for 1 h. The redox properties of the modified electrodes were investigated using cyclic voltammetry in acetonitrile (0.1 M Bu_4NPF_6). The electrolyte solution was rigorously purged with N_2 for 2 min before the voltammetry data were recorded. The surface coverage (Γ in mol cm^{-2}) of the electropolymerized material (for films deposited from 16 scan cycles) was estimated by integrating the charge under the cyclic voltammetric wave for the first reduction wave of the cyclophane moiety. In these calculations, we assumed that this wave was due to a two-electron reduction.

Acknowledgements

We thank the EPSRC for funding this work and Rikagu for the loan of a diffractometer.

References and notes

1. For an early report of this macrocycle, see: Odell, B.; Reddington, M. V.; Slawin, A. M. Z.; Spencer, N.; Stoddart, J. F.; Williams, D. J. *Angew. Chem., Int. Ed. Engl.* **1988**, *27*, 1547–1550.
2. For recent reviews that include $CBPQT^{4+}$ based devices, see: (a) Pease, A. R.; Jeppesen, J. O.; Stoddart, J. F.; Luo, Y.; Collier, C. P.; Heath, J. R. *Acc. Chem. Res.* **2001**, *34*, 433–444; (b) Flood, A. H.; Liu, Y.; Stoddart, J. F. *Modern Cyclophane Chemistry*; Hopf, H., Gleiter, H., Eds.; Wiley-VCH: Weinheim, 2004; pp 485–518.
3. For a recent review featuring $CBPQT^{4+}$ moieties immobilized at surfaces, see: Braunschweig, A. B.; Northrop, B. H.; Stoddart, J. F. *J. Mater. Chem.* **2006**, *16*, 32–44.
4. For representative examples of electropolymerized interlocked structures, see: (a) Zhou, S. S.; Carroll, P. C.; Swager, T. M. *J. Am. Chem. Soc.* **1996**, *118*, 8713–8714; (b) Zhou, S. S.; Swager, T. M. *J. Am. Chem. Soc.* **1997**, *119*, 12568–12577; (c) Vidal, P. L.; Billon, M.; Divisia-Blohorn, B.; Bidan, G.; Kern, J. M.; Sauvage, J. P. *Chem. Commun.* **1998**, 629–630; (d) Billon, M.; Divisia-Blohorn, B.; Kern, J.-M.; Sauvage, J.-P. *J. Mater. Chem.* **1997**, *7*, 1169–1173; (e) Simone, D. L.; Swager, T. M. *J. Am. Chem. Soc.* **2000**, *122*, 9300–9301; (f) Cooke, G.; Garety, J. F.; Mabruk, S.; Rabani, G.; Rotello, V. M.; Surpateanu, G.; Woisel, P. *Tetrahedron Lett.* **2006**, *47*, 783–786.
5. Cooke, G.; Garety, J. F.; Jordan, B.; Kryvokhyzha, N.; Parkin, A.; Rabani, G.; Rotello, V. M. *Org. Lett.* **2006**, *8*, 2297–2300.
6. Cooke, G.; Woisel, P.; Bria, M.; Delattre, F.; Garety, J. F.; Hewage, S. G.; Rabani, G.; Rosair, G. M. *Org. Lett.* **2006**, *8*, 1423–1426.
7. Pickett, C. J.; Ryder, K. S. *J. Chem. Soc., Dalton Trans.* **1994**, 2181–2189.
8. Asakawa, M.; Dehaen, W.; L'Abbé, G.; Menzer, S.; Nouwen, J.; Raymo, F. M.; Stoddart, J. F.; Williams, D. J. *J. Org. Chem.* **1996**, *61*, 9591–9595.
9. Bravo, J. A.; Raymo, F. M.; Stoddart, J. F.; White, A. J. P.; Williams, D. J. *Eur. J. Org. Chem.* **1998**, 2565–2571.
10. Hamilton, D. G.; Davies, J. E.; Prodi, L.; Sanders, J. K. M. *Chem.—Eur. J.* **1998**, *4*, 608–620.
11. (a) Ashton, P. R.; Brown, C. L.; Chrystal, E. J. T.; Goodnow, T.; Kaifer, A. E.; Parry, K. P.; Philp, D.; Slawin, A. M.; Spencer, N.; Stoddart, J. F.; Williams, D. J. *J. Chem. Soc., Chem. Commun.* **1991**, 634–639; (b) Ashton, P. R.; Goodnow, T. T.; Kaifer, A. E.; Reddington, M. V.; Slawin, A. M. Z.; Spencer, N.; Stoddart, J. F.; Vicent, C.; Williams, D. J. *Angew. Chem., Int. Ed. Engl.* **1989**, *28*, 1396–1399.
12. Anelli, P. L.; Ashton, P. R.; Ballardini, R.; Balzani, V.; Delgado, M.; Gandolfi, M. T.; Goodnow, T. T.; Kaifer, A. E.; Philp, D.; Pietraszkiewicz, M.; Prodi, L.; Reddington, M. V.; Slawin, M. V.; Spencer, A. M. Z.; Stoddart, J. F.; Vicent, C.; Williams, D. J. *J. Am. Chem. Soc.* **1992**, *114*, 193–218.
13. Aprahamian, I.; Dichtel, W. R.; Ikeda, T.; Heath, J. R.; Stoddart, J. F. *Org. Lett.* **2007**, *9*, 1287–1290.
14. Wu, Q.; Storrier, G. D.; Wu, K. R.; Shapeleigh, J. P.; Abruña. *Anal. Biochem.* **1998**, *263*, 102–112.
15. Jeppesen, J. O.; Nielsen, K. A.; Perkins, J.; Vignon, S. A.; Di Fabio, A.; Ballardini, R.; Gandolfi, M. T.; Venturi, M.; Balzani, V.; Becher, J.; Stoddart, J. F. *Chem.—Eur. J.* **2003**, *9*, 2982–3007.
16. (a) Loveland, J. W.; Dimeler, G. R. *Anal. Chem.* **1961**, *33*, 1196–1201; (b) D'Elia, L. F. D.; Ortiz, R. *Port. Electrochim. Acta* **2005**, *23*, 481–490; (c) D'Elia, L. F.; Ortiz, R. L. *J. Electrochem. Soc.* **2006**, *153*, D187–D192.
17. For examples of pseudorotaxane-based conducting polymers, see: (a) Marsella, M. J.; Carroll, P. J.; Swager, T. J. *J. Am. Chem. Soc.* **1994**, *116*, 9347–9348; (b) Marsella, M. J.; Carroll, P. J.; Swager, T. J. *J. Am. Chem. Soc.* **1995**, *117*, 9832–9841.
18. Brown, C. L.; Philp, D.; Spencer, N.; Stoddart, J. F. *Isr. J. Chem.* **1992**, *32*, 61–67.
19. Rigaku, 9009 New Trails Drive, The Woodlands, TX 77381, USA.
20. Farrugia, L. J. *J. Appl. Crystallogr.* **1999**, *32*, 837–838.
21. Altomare, A.; Cascarano, G.; Giacovazzo, C.; Guagliardi, A. *J. Appl. Crystallogr.* **1993**, *26*, 343–350.
22. Betteridge, P. W.; Carruthers, J. R.; Cooper, R. I.; Prout, K.; Watkin, D. J. *J. Appl. Crystallogr.* **2003**, *36*, 1487.
23. Allen, F. H. *Acta Crystallogr.* **2002**, *B58*, 380–388.